Model simulations of a reflective semiconductor optical amplifier at modulation speeds up to 10 Gb/s

M. van Iersel, D. Lenstra, and K. Allaart

COBRA research institute, Vrije Universiteit,

De Boelelaan 1081, 1081 HV Amsterdam, the Netherlands

We develop a model and perform simulations on the basis of rate equations for a reflective semiconductor optical amplifier. The latter will be used as part of a transceiver device for fiber-to-the-home applications. Simulation results for bulk amplifiers will be presented and discussed both for the static and dynamic performance. We will focus on a modulation scheme and the highest speed of modulation that can be achieved.

Model

The semiconductor optical amplifier (SOA) modulator we consider, is a reflective amplifier with bulk material as the active element and a total round-trip length L. The signal entering the SOA is a CW-signal which is electrically modulated inside the device. We assume that there is only one reflection, i.e., at the back of the device. A sketch of the reflective amplifier is given in Fig. 1 together with the relevant electric fields. Here r is

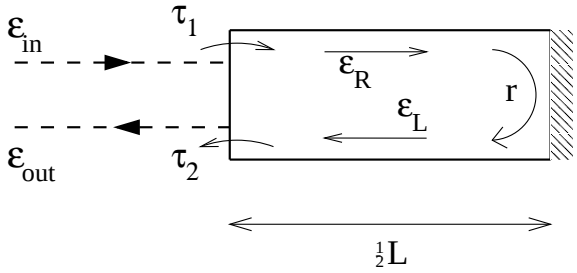

Figure 1: Drawing of the amplifier and the electric fields involved.

the reflection coefficient at the back of the device and τ_1 and τ_2 are the transmission coefficients of a wave entering resp. leaving the device. The incoming and outgoing electric fields are denoted by $\mathcal{E}_{in}$ and $\mathcal{E}_{out}$. The internal electric field consists of two fields, one running to the right, $\mathcal{E}_R$, and one running to the left, $\mathcal{E}_L$.
We have modeled the SOA using a rate equation for the inversion and an expression for the outgoing field in terms of the incoming field and the instantaneous inversion. This last equation (nonlinear gain included) is given by

$$E_{out}(t) \;=\; r\tau_1\tau_2 \exp\left[\frac{1}{2}(1+i\alpha)\frac{\xi}{1+\varepsilon\langle|\,E(t)\,|^2\rangle}\frac{L}{v_g}N(t)\right]E_{in}\,. \qquad (1)$$

Here ξ is the gain coefficient, α the detuning parameter, v_g the group velocity in the bulk material and $N(t)$ the total inversion. The change in inversion around the point of transparency (including nonlinear gain) is given by

$$\frac{\mathrm{d}}{\mathrm{d}t}N(t) \;=\; J(t) - J_{trans} - \frac{N(t)}{T_1} - \frac{\xi}{1+\varepsilon\langle|\,E(t)\,|^2\rangle}N(t)\langle|\,E(t)\,|^2\rangle\,. \qquad (2)$$

In Eqs. (1) and (2) the quantity $\langle \mid E(t) \mid^2 \rangle$ represents the averaged total internal intensity carried by the right and left traveling waves in the amplifier. We have taken these directional intensities exponentially growing in the propagation direction. The rate at which carriers are injected in the active region is given by the pump current $J(t)$ and the transparency current J_{trans}. The third term in Eq. (2) gives all recombination processes except stimulated emission. Note that this term is an approximation (see e.g. [1]). The life time for spontaneous recombination of electrons and holes is denoted by T_1. The last term in Eq. (2) gives the stimulated emission.

Numerical calculation

It is quite common to consider the output power instead of the outgoing electric field, which are related via $P_{out}(t) = \mid E_{out}(t) \mid^2$. Using this relation we can rewrite the equation for the outgoing electric field, Eq. (1),

$$P_{out}(t) \;=\; r^2\tau_1^2\tau_2^2 \exp\left[\frac{\xi}{1+\varepsilon\langle \mid E(t) \mid^2\rangle}\frac{L}{v_g}N(t)\right]E_{in}^2\,. \tag{3}$$

It is this equation together with Eq. (2) that is solved numerically by using a fourth-order Runge-Kutta method [2] for the first-order differential equation for the inversion.
As input parameter we do not use the gain coefficient ξ, but we use the cross section for the transition g instead. These two are related by $\xi L = g v_g/A$. We have chosen to use g because it is a material constant, as are the group velocity and the cross section of the active region. Whereas ξ is only a constant in the product with L and not by itself.

CW analysis

Firstly, we consider the case of a constant pump current, i.e., no modulation. The calculations showed that the results for linear and nonlinear gain smoothly connect to each other. We studied the dependence of the transmission as a function of the input power, see Fig. 2. The calculations are done for several values of the pump current $J(t)$, a transparency current of 30 mA, a round-trip length of 1 mm and a nonlinear gain coefficient $\varepsilon = 10^{-8}$. Fig. 2 shows a large transmission for small values of the input power and a

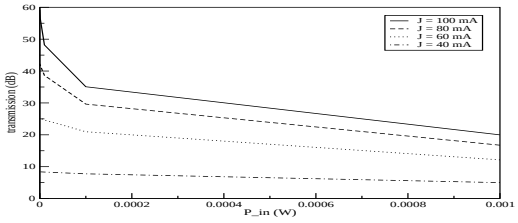

Figure 2: Transmission vs. input power calculated for several values of the pump current. $J_{trans} =$ 30 mA, $\varepsilon = 10^{-8}$, $L = 1$ mm.

saturation of the transmission for increasing values of the input power. We also observed that an increasing pump current or decreasing current at transparency causes an increase in the transmission.

Another parameter dependence we investigated is the influence of the round-trip length on the transmission. One has to realize that the pump current and current at transparency should be scaled inversely to the length. This way the number of electrons inside the device stays equal and it is possible to see the influence of the length on the transmission. In our calculations we started with a round-trip length $L = 1$ mm, a pump current $J = 10$ mA and a current at transparency $J_{trans} = 8$ mA. The length was decreased up down to 0.1 mm and the other parameters scaled accordingly. The calculations are done at several values of the input power. The results are plotted in Fig. 3, where we have used

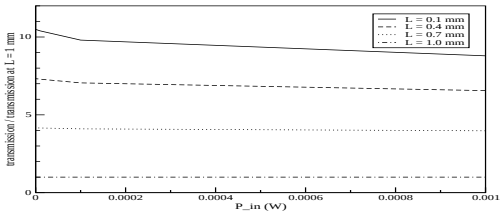

Figure 3: Transmission divided by the transmission at $L = 1$ mm vs. the input power for several values of the round-trip length. J and J_{trans} are inversely scaled with L.

the transmission divided by the transmission at length $L = 1$ mm (i.e., the scaling factor), instead of just the transmission. For all lengths except 1 mm we see that the curves deviate somewhat from their ideal value of the scaling factor; at small input powers the curves lie above the ideal value and at large input powers they lie beneath it, where the deviation becomes larger when the scaling factor increases.

Modulation properties

In the next step we have included modulation in our calculations, where a simple on/off-scheme was studied. Fig. 4 shows the results of the calculations at a bit rate of 1 Gb/s for different values of the pump current in the 'on'-state while the 'off'-state is kept at 0 mA. Nice bit patterns are observed only for higher values of the pump current. Similar

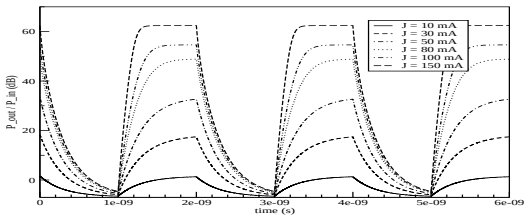

Figure 4: Transmission vs. time for different values of the pump current in the 'on'-state. $J_{off} = 0$ mA, $J_{trans} = 8$ mA, $P_{in} = 10^{-5}$ W, $\varepsilon = 10^{-8}$.

calculations (also 1 Gb/s) were performed when varying the input power and using a pump current $J_{on} = 100$ mA. Again, nice bit patterns are obtained only for larger values of the input power.

In the previous calculations we have determined reasonable parameter values for the input power, $P_{in} = 10^{-5}$ W, and the current in the 'on'-state, $J_{on} = 100$ mA. These values were

used when investigating the influence of the data speed on the transmission, with the data rate varied from 0.1 Gb/s up to 10 Gb/s. In Fig. 5 the results are shown. We see that the

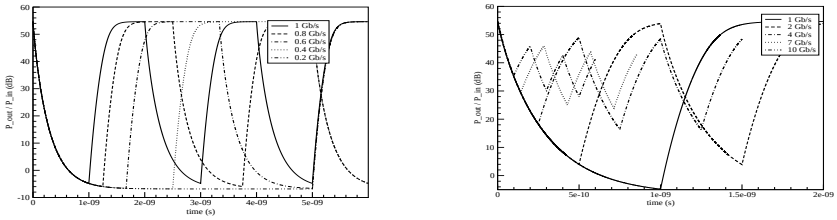

Figure 5: Transmission vs. time for data rates in the range of 0.1 Gb/s to 1 Gb/s (left graph) and 1 Gb/s to 10 Gb/s (right graph).

bit-pattern quality decreases when the data speed increases. For a better understanding of the changes in transmission we have plotted the third minimum and maximum value of the transmission. These values are plotted in Fig. 6. A good extinction ratio (> -20 dB) is found for speeds up to 6 Gb/s.

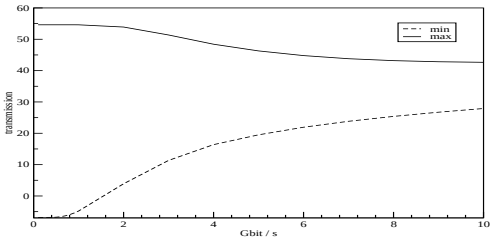

Figure 6: Value of transmission of the third minimum and maximum vs. the data rate.

Conclusions and outlook

For an incoming CW-signal and constant pump current we found saturation of the transmission at $P_{in} \approx 0.1$ mW (at $J = 100$ mA). When electrically modulating this signal we found nice bit patterns at values larger than those mentioned above. We also found a good extinction ratio for modulation speeds up to 6 Gb/s.
In future work noise due to amplified spontaneous emission will be included for the bulk material amplifier. Also SOAs with quantum dot active material will be investigated.

Acknowledgments

This work is part of the Freeband BBphotonics project (http://bbphotonics.freeband.nl). Freeband is sponsored by the Dutch government under contract BSIK 03025.

References

[1] G.P. Agrawal and N.K. Dutta, Semiconductor Lasers, New York: Van Nostrand Reinhold, 1993

[2] W.H. Press, S.A. Teukolsky, W.T. Vetterling and B.P. Flannery, Numerical recipes in Fortran, Cambridge: Cambridge University Press, 1992